Inorganic Chemistry

Article

Cite This: Inorg. Chem. 2017, 56, 14999−15005

pubs.acs.org/IC

Cation-Exchanged Zeolitic Chalcogenides for CO_2 Adsorption

Huajun Yang,[†,⊥] Min Luo,[†,⊥] Xitong Chen,[‡,⊥] Xiang Zhao,[§] Jian Lin,[†] Dandan Hu,[†] Dongsheng Li,[∥] Xianhui Bu,[§] Pingyun Feng,*[,‡] and Tao Wu*[,†]

[†]College of Chemistry, Chemical Engineering and Materials Science, Soochow University, Suzhou, Jiangsu 215123, China

[‡]Department of Chemistry, University of California, Riverside, California 92521, United States

[§]Department of Chemistry and Biochemistry, California State University, Long Beach, California 90840, United States

[∥]College of Materials and Chemical Engineering, Hubei Provincial Collaborative Innovation Center for New Energy Microgrid, Key Laboratory of Inorganic Nonmetallic Crystalline and Energy Conversion Materials, China Three Gorges University, Yichang, Hubei 443002, China

Supporting Information

ABSTRACT: We report here the intrinsic advantages of a special family of porous chalcogenides for CO_2 adsorption in terms of high selectivity of CO_2/N_2, large uptake capacity, and robust structure due to their first-ever unique integration of the chalcogen-soft surface, high porosity, all-inorganic crystalline framework, and the tunable charge-to-volume ratio of exchangeable cations. Although tuning the CO_2 adsorption properties via the type of exchangeable cations has been well-studied in oxides and MOFs, little is known about the effects of inorganic exchangeable cations in porous chalcogenides, in part because ion exchange in chalcogenides can be very sluggish and incomplete due to their soft character. We have demonstrated that, through a methodological change to progressively tune the host−guest interactions, both facile and nearly complete ion exchange can be accomplished. Herein, a series of cation-exchanged zeolitic chalcogenides (denoted as M@RWY) were studied for the first time for CO_2 adsorption. Samples were prepared through a sequential ion-exchange strategy, and Cs^+-, Rb^+-, and K^+-exchanged samples demonstrated excellent CO_2 adsorption performance. Particularly, K@RWY has the superior CO_2/N_2 selectivity with the N_2 adsorption even undetected at either 298 or 273 K. It also has the large uptake of 6.3 mmol/g (141 cm^3/g) at 273 K and 1 atm with an isosteric heat of 35−41 kJ mol^{-1}, the best among known porous chalcogenides. Moreover, it permits a facile regeneration and exhibits an excellent recyclability, as shown by the multicycling adsorption experiments. Notably, K@RWY also demonstrates a strong tolerance toward water.

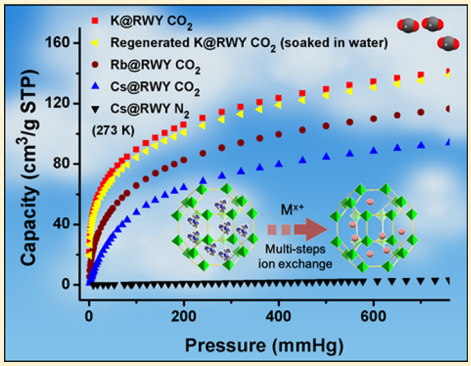

INTRODUCTION

The increasing level of atmospheric CO_2, largely correlated to the combustion of fossil fuels, is currently a very pressing environmental concern.[1] Among the few and yet viable strategies that can deal with the emission of CO_2 is carbon capture and storage (CCS).[2] Currently, the most mature and commercially available technology for CCS is "wet scrubbing" methods based on chemical reactions between CO_2 and amines in aqueous solutions.[3] Though this technology is straightforward to apply, the high energy demand for the regeneration of the amines is a major problem.[4] Alternatively, capture of CO_2 based on porous solid adsorbents has the potential to perform such a capture at a much reduced energy penalty and has therefore received much attention in recent years.[5]

Many different porous solid materials have been investigated, including oxide-based zeolites,[6−9] aluminophosphates,[10−12] porous carbons,[13,14] porous organics,[15,16] and metal−organic frameworks (MOFs).[17−22] Generally, the practical CO_2 adsorption requires the sorbents to possess large uptake capacity, high selectivity, facile recyclability, and also excellent stability (especially when exposed to water vapor). Unfortunately, it seems that the "perfect" sorbents that can satisfy all the requirements still remain elusive. For example, the well-developed zeolite 13X is very stable and has a high selectivity, but its uptake capacity is relatively low.[23] On the contrary, MOF-74s, a very popular series of MOFs, have the record-high uptake capacity and a high selectivity for CO_2 over N_2.[24] However, the presence of water vapor can reduce their gas uptake capacity significantly and can degrade or even destroy the crystal structure, restricting their practical use.[25,26] It is thus very important to search for new sorbent materials.

Recently, chalcogenide porous materials including chalcogels and zeolitic chalcogenides have attracted widespread attention in the field of CO_2 adsorption because of their inorganic frameworks and the soft surface of electron-rich chalcogenide atoms.[27−30] The polarizability of porous chalcogenides is therefore much higher than that of oxide frameworks and porous organics, rendering a strong affinity toward highly polarizable species, such as CO_2 (polarizability (α): $\alpha(CO_2)$ =

Received: September 7, 2017
Published: December 1, 2017

© 2017 American Chemical Society

DOI: 10.1021/acs.inorgchem.7b02307
Inorg. Chem. 2017, 56, 14999−15005

2.51 cm^{-3}), based on the hard and soft acid−base theory (HSAB).[31,32] For examples, Kanatzidis et al. found that mesoporous germanium-rich chalcogenide frameworks exhibited excellent selectivity for separating hydrogen from carbon dioxide and methane.[33] We also found that the Cs^+-exchanged form of a zeolitic chalcogenide analogue (CPM-120) showed CO_2 adsorption with high capacity and affinity (98 cm^3/g at 273 K, isosteric heat of 40.05 kJ mol^{-1}).[30] These results demonstrate that porous chalcogenides have the potential to act as excellent CO_2 adsorbing materials that integrate stability with high selectivity for CO_2 over other gases.

Here, we focus our study on the charge-balancing cations in the channel of the frameworks. We show that this is an effective strategy to improve the CO_2 adsorption. In fact, the impact of charge-balancing inorganic cations on gas adsorption is known in both zeolites and MOFs.[34−37] However, this strategy has not been realized in porous chalcogenides, which is probably due to the rather limited exchange (highly selective for "soft" cations) in porous chalcogenides arising from their "soft" character.[38] Recently, targeting nuclear waste remediation, we developed a strategy based on amine−Cs−K ion exchange and reverse K−Cs ion exchange in 3D zeotype chalcogenides (UCR-20, denoted as RWY in the database of zeolite structures).[39] In this work, we systematically synthesized a series of cation-exchanged zeolitic chalcogenides (M@RWY) and extensively studied their capacity and selectivity for CO_2 capture. The results showed that the K^+-exchanged RWY had the best performance for CO_2 adsorption.

EXPERIMENTAL SECTION

Syntheses. The pre-ion-exchanged solid samples of UCR-20-GaGeS ($[Ga_xGe_{4-x}S_8]^{x-}$, also named PA@RWY) were synthesized according to the literature method.[38]

Stepwise Ion-Exchange Strategy. The stepwise ion-exchange strategy consists of the following steps.

Step 1. The protonated amines (PAs) were first exchanged out by "soft" Cs^+. Typically, a 500 mg portion of pristine RWY crystals is soaked in 100 mL of CsCl aqueous solution (1 M) in a glass vial, which was sealed and subsequently put in an 85 °C oven. The CsCl solution was refreshed once during treatment. After 48 h, the crystals (named as Cs@RWY) were washed by deionized water and ethanol several times, and dried in vacuum. The process can be described as follows:

$$Cs^+ + PA@RWY \xrightarrow{85\ ^\circ C} Cs@RWY + PA^+ \ (PA = \text{protonated amine}) \quad (1)$$

Step 2A. A 100 mg portion of Cs@RWY crystals was immersed in 100 mL of RbCl solution (1 M) at room temperature. The solution was refreshed once with a total time of around 48 h to remove Cs^+ ions in the channels of RWY. Subsequently, the samples (named as Rb@RWY) were washed by deionized water and ethanol, and dried in a vacuum oven. The ion-exchange process can be described as follows:

$$Rb^+ + Cs@RWY \xrightarrow{RT} Rb@RWY + Cs^+ \quad (2A)$$

Step 2B. A 100 mg portion of Cs@RWY crystals was immersed in 100 mL of KCl solution (2 M) at room temperature (RT). The solution was refreshed once with a total time of around 48 h to remove Cs^+ ions in the channels of RWY. Subsequently, the crystals (named as K@RWY) were washed by deionized water and ethanol several times, and dried in a vacuum oven. The ion-exchange process was expressed as

$$K^+ + Cs@RWY \xrightarrow{RT} K@RWY + Cs^+ \quad (2B)$$

Step 3. A 100 mg portion of K@RWY crystals was immersed in 100 mL of MCl_x solution (M = Na^+, Mg^{2+}, Ca^{2+}, Sr^{2+}) at room temperature. The solution was refreshed twice with a total time of around 48 h to remove K^+ ions in the channels of RWY completely. Subsequently, the samples (named as M@RWY) were washed by deionized water and ethanol, and dried in a vacuum oven. The ion-exchange process was expressed as

$$M^{x+} + K@RWY \xrightarrow{RT} M@RWY + K^+ \quad (3)$$

Gas Adsorption Experiments. The CO_2 and N_2 adsorption isotherms of cation-exchanged samples were recorded using a Micromeritics ASAP 2020 physisorption analyzer. The cation-exchanged samples were dried in the vacuum oven for 4 h and were further degassed for 10 h at 373 K. CO_2 adsorption isotherms were recorded at 273, 298, and 313 K, and the temperature of the experiments was controlled by a Dewar flask.

Evaluation of CO_2 Capture Performance. To evaluate the CO_2 capture performance of the ion-exchanged zeolitic RWY materials, measured CO_2 and N_2 isotherms were fit with adsorption models. Simple adsorption models, such as the single-site Langmuir (SSL) model, often do not adequately describe CO_2 adsorption on heterogeneous surfaces. As such, a dual-site Langmuir (DSL) model was employed to describe the CO_2 adsorption of ion-exchanged RWY zeolite materials over the entire pressure range:

$$N = N_A + N_B = \frac{N_{A,sat.}k_A p}{1 + k_A p} + \frac{N_{B,sat.}k_B p}{1 + k_B p} \quad (5)$$

where N is the quantity adsorbed, p is the pressure of bulk gas at equilibrium with adsorbed phase, $N_{A,sat.}$ and $N_{B,sat.}$ are the saturation loadings for sites A and B, and k_A and k_B are the Langmuir parameters for sites A and B, respectively.

To estimate the CO_2/N_2 separation performance of Cs@RWY under conditions relevant to CO_2 capture, ideal adsorbed solution theory (IAST) was used to calculate the selectivity of CO_2 over N_2.[40] The detailed methodology for calculating the amount of CO_2 and N_2 adsorption from a mixture is described elsewhere.[41] The accuracy of the IAST procedure has already been established for adsorption of a wide variety of gas mixtures in many different zeolites. The adsorption selectivity is defined as

$$\text{selectivity} = \frac{q_A/q_B}{p_A/p_B} \quad (6)$$

where q_i is the uptake quantity and p_i is the partial pressure of component i.

The isosteric heats of adsorption for CO_2 were calculated using the DSL isotherm fits at 273 and 298 K. The isosteric heat of CO_2 adsorption was calculated by following the Clausius−Clapeyron equation.

RESULTS AND DISCUSSION

Preparation of Cation-Exchanged Samples through Stepwise Ion-Exchange Strategy. The structure of RWY is constructed from supertetrahedral T2 ($[Ga_xGe_{4-x}S_{10}]$) clusters with sodalite topology by treating the clusters as nodes (Figure S1). Disordered positively charged amines, protonated tris(2-dimethyl-aminoethyl) amine (TAEA), are located in the channels. The pristine zeolitic chalcogenides (amine@RWY) showed negligible gas adsorption due to the pore blockage by the bulky templating amines.

To investigate the effect of the charge-balancing cations on the gas adsorption properties of the porous zeolitic chalcogenides, the protonated amine in pristine RWY was postsynthetically exchanged with Cs^+, Rb^+, K^+, Na^+, Sr^{2+}, Ca^{2+}, and Mg^{2+}, which afforded Cs@RWY, Rb@RWY, K@RWY, Na@RWY, Sr@RWY, Ca@RWY, and Mg@RWY, respectively. The experiments were performed by immersing the crystals in

DOI: 10.1021/acs.inorgchem.7b02307
Inorg. Chem. 2017, 56, 14999−15005

the aqueous solutions of various hydrated metal salts. Notably, extra ion-exchange processes are needed in order to make more complete exchange except with the use of Cs^+. This could be because the RWY framework with "soft" character has a strong affinity toward "soft" cations (e.g., Cs^+) and a weak affinity toward "hard" cations (e.g., K^+). For example, we can obtain nearly fully Cs^+ activated samples (Cs@RWY) through a single-step ion-exchange process. (The exchange degree is calculated by the reduction of protonated amines based on the content of N from CHN elemental analysis, as shown in Table S1.) In comparison, only 61% of organic amines can be directly exchanged out by K^+ and 48% by Na^+.[38] Actually, the Cs^+ ions in Cs@RWY can be nearly fully expelled from RWY with excess K^+ but not with Na^+ due to the relatively small polarizability of Na^+. The fully Na^+ activated samples (Na@RWY) could only be obtained from K@RWY with two successive steps as Cs@RWY → K@RWY → Na@RWY, shown in Scheme 1.

Scheme 1. Stepwise Ion-Exchange Processes for Various Cation-Exchanged Samples

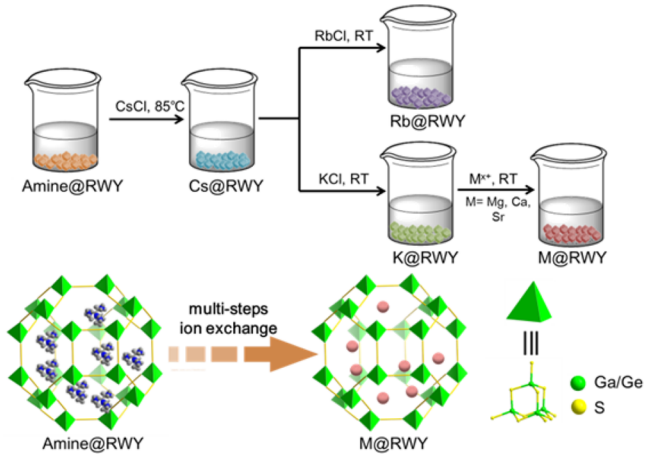

Through the stepwise ion-exchange processes as shown in Scheme 1, a series of cation-exchanged samples were successfully synthesized including Cs@RWY, Rb@RWY, K@RWY, Na@RWY, Mg@RWY, Ca@RWY, and Sr@RWY (Figure S2). The ion-exchange processes were demonstrated to be basically complete on the basis of the fact that EDS experiments cannot detect any residual of the original cations (Figure S3). The contents of Cs in Rb@RWY and K@RWY were further analyzed by ICP-MS by digesting the samples. The results indicated that the exchange degrees for Rb@RWY and K@RWY were 93.8% and 97.3%, respectively. The PXRD peaks of the pristine samples and as-exchanged samples can be well-indexed with those in the simulated one, indicating that all the samples have the pure phase and the exchanged samples maintained the parent framework after ion-exchange processes (Figure 1). The unit cells from SCXRD also indicated the shrink of the lattice from pristine RWY to Cs@RWY, to Rb@RWY, and to K@RWY, following the order of the balanced species' size (Figure S4). Notably, the diffraction peaks for the divalent metal cation-exchanged samples have an obvious shift toward a larger angle, compared with those of other samples. This is reasonable because, by replacing monovalent cations with divalent cations, the amount of cations as the charge-balancing species in the framework is reduced by half. The higher charge and smaller number of the cations are responsible

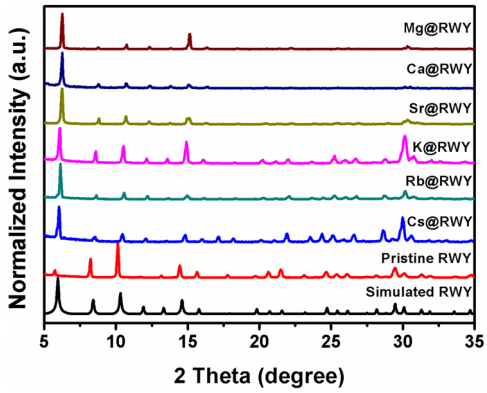

Figure 1. PXRD patterns of the various cation-exchanged samples.

for the shrinkage of the crystal lattice. Unfortunately, due to the bad quality of the divalent-cations-exchanged crystals, it cannot be demonstrated directly by SCXRD analysis.

Surface Area Characterizations. There exists a large amount of water molecules in the channels of ion-exchanged samples including Cs@RWY and K@RWY, which need to be removed by a degassing process before the gas adsorption analysis. The degassing processes were typically performed at 373 K for 10 h. PXRD measurements indicated that the samples of Cs@RWY, Rb@RWY, and K@RWY could retain the pristine structure after degassing treatment but Na@RWY, Mg@RWY, Ca@RWY, and Sr@RWY could not retain the crystallinity (even at 313 K) (Figures S5–S6). As such, the samples of Na@RWY, Mg@RWY, Ca@RWY, and Sr@RWY did not exhibit porosity. For the situation in Ca@RWY, Sr@RWY, and Mg@RWY, the instability is perhaps due to the larger void spaces in these samples induced by the greatly reduced amount of the charge-balancing cations (Mg^{2+}, Ca^{2+}, and Sr^{2+}), compared with those in Cs@RWY, Rb@RWY, and K@RWY. For Na@RWY, it may be related to the weak interaction between Na^+ and the framework, and the precise reason still requires further study. As a result, in this work, only the gas adsorption properties of the latter ones were characterized and studied.

To investigate the surface areas of the activated samples, N_2 adsorption measurements were performed at 77 K. As shown in Figure 2a, all the samples were found to exhibit typical type-I adsorption isotherms and steep N_2 uptake in the low-pressure regions ($P/P_0 < 0.05$), indicating the microporosity of these materials. The Brunauer–Emmett–Teller (BET) surface areas of Cs@RWY, Rb@RWY, and K@RWY were calculated to be 526, 638, and 716 m^2/g, respectively. The pore volume was found to increase from 0.277, to 0.363, to 0.381 cc g^{-1}, respectively. The pore size distributions, as calculated by the Horvath–Kawazoe method, indicated that the exchanged cations had little effect on the pore size (Figure 2b). The median pore size of all the exchanged samples was found to be nearly the same with the value of 0.62 nm. As a result, the increase of the BET surface areas from Cs@RWY to K@RWY is believed to be mainly caused by the decrease of the formula weight and cation sizes rather than the increase of the pore size.

Selectivity of CO_2 Adsorption. The CO_2 adsorption isotherms at 273, 298, and 313 K for Cs@RWY, Rb@RWY, and K@RWY are shown in Figure 3a and Figures S8–S10. The relatively high uptake is observed in all the samples, with the order following Cs@RWY < Rb@RWY < K@RWY. K@RWY exhibits the highest capacity of 86.7 cm^3/g (3.87 mmol/g) at

DOI: 10.1021/acs.inorgchem.7b02307
Inorg. Chem. 2017, 56, 14999–15005

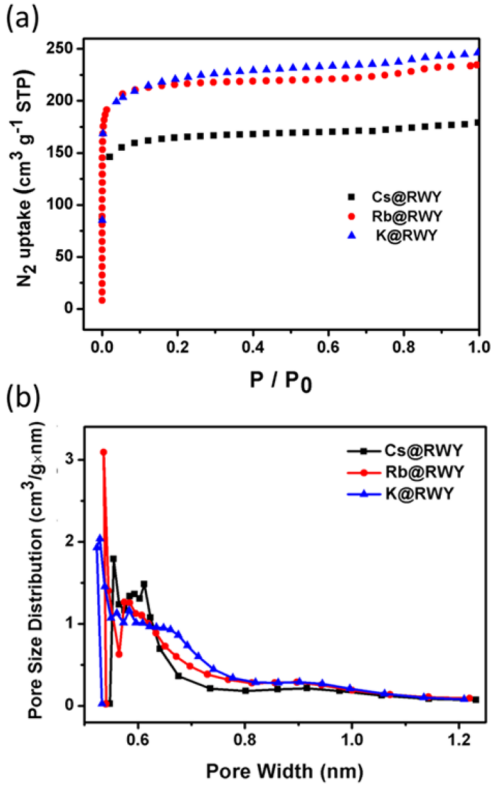

Figure 2. (a) N_2 adsorption isotherms of Cs@RWY, Rb@RWY, and K@RWY. (b) Pore size distributions of Cs@RWY, Rb@RWY, and K@RWY calculated by the Horvath−Kawazoe method.

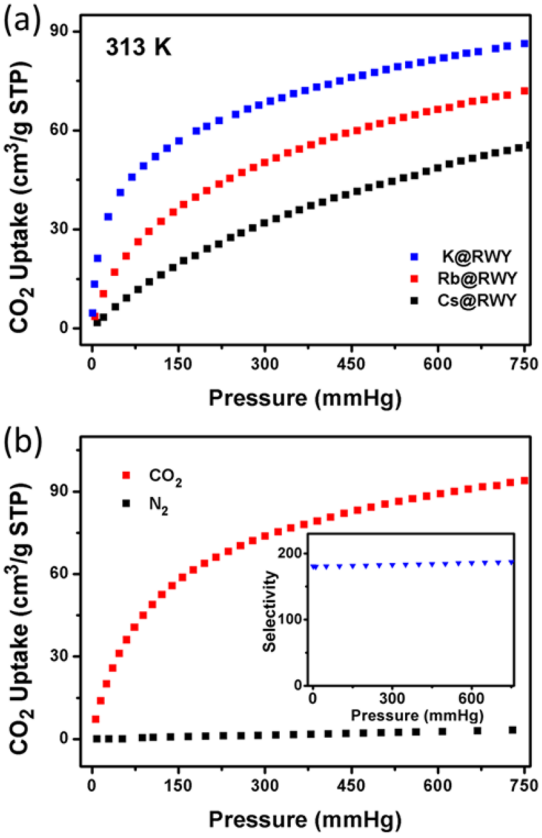

Figure 3. (a) CO_2 adsorption isotherms of Cs@RWY, Rb@RWY, and K@RWY at 313 K. (b) Adsorption isotherms of Cs@RWY for CO_2 and N_2 at 273 K. Inset shows the CO_2/N_2 selectivity calculated by IAST theory.

313 K and 1 atm. Due to the difference in the formula weight of the as-exchanged samples, it is thus more reasonable to compare the volumetric capacity. The calculated results revealed that the volumetric capacity of all the samples still exhibited the increasing trend from Cs@RWY to K@RWY, indicating the stronger affinity toward CO_2 for K@RWY. Notably, the previously studied porous chalcogenides (mostly chalcogels) have a high selectivity for CO_2 capture. However, one issue for those chalcogels is their small capacity for CO_2 uptake (<1 mmol/g), as shown in Table 1. The uptake capacity reported here represents the highest value among chalcogenides, which is also higher than that of commercialized oxide zeolite (NaX). The volumetric uptake value is also comparable to the MOF-74 series.

To better understand the affinities toward CO_2 of the as-exchanged samples, the adsorption heat (Q_{st}) was calculated on the basis of the Clausius−Clapeyron equation. All of the adsorption isotherms were well-fitted based on the dual-site Langmuir model (Tables S2−S4). This could be ascribed to the existence of two kinds of surface sulfur sites in a T2 unit, that is, four core-sulfur sites and six edge-sulfur sites (Figure S1). It was found that the low coverage of the Q_{st} values increased from Cs@RWY (30.2−32.1 kJ mol^{-1}) to K@RWY (35.0−41.1 kJ mol^{-1}) (Figure S11 and Table 1). The affinity gap of the exchanged samples could be explained as follows. For cation-exchanged RWY, even though the location of the charge-balancing cations could not be determined by single-crystal structure analysis, they should be present near the surface of the framework due to the electrostatic interactions, similar to the situation in oxide zeolites. K^+, with a higher charge-to-volume ratio than Rb^+ and Cs^+, may have a stronger interaction with CO_2, which contributed to its higher Q_{st}. Also, the adsorption mechanism in these materials should include the strong interaction of "soft" CO_2 and "soft" exposed framework sulfur sites. For such interactions, the large near-surface Cs^+ sites provide greater steric hindrance for the access of CO_2 to the sulfur sites.

Due to the high uptake and strong interaction for CO_2 adsorption, we were motivated to test the CO_2/N_2 selectivity of the samples. Remarkably, the values of the CO_2/N_2 selectivity are impossible to determine validly under ambient temperature (298 K) because the N_2 adsorption of all three samples is essentially zero despite the various efforts we have made, indicative of extraordinarily high selectivity. The negligible adsorption of N_2 persists for K^+ and Rb^+ samples even down to 273 K. Eventually we were able to achieve a measurable, yet very low, amount of N_2 adsorption of Cs@RWY (Figure S12). The adsorption isotherms of CO_2 and N_2 at 273 K for Cs@RWY were shown in Figure 3b, in which a high amount of CO_2 uptake and a very small amount of N_2 uptake were observed, indicating a high CO_2/N_2 selectivity. The ideal adsorbed solution theory (IAST), a widely adopted method to predict a mixed isotherm from a pure gas isotherm, was then employed to determine the selectivity of CO_2 over N_2. The predicted selectivity in a mixture of 15% CO_2 and 85% N_2 in a molar ratio under different pressures is shown in the inset of Figure 3b. The value is found to be around 180, higher than that of the commercialized oxide zeolite materials and approximately equal to that of MOF-74. All of these results demonstrated the extraordinarily high CO_2/N_2 selectivity of cation-exchanged zeolitic chalcogenide materials.

DOI: 10.1021/acs.inorgchem.7b02307
Inorg. Chem. 2017, 56, 14999−15005

Table 1. Comparison of CO_2 Adsorption Capacity and IAST-Calculated Selectivity for the 15%/85% CO_2/N_2 Mixture in Different Porous Materials at 298 K[23,24,28,42−46]

material	adsorption enthalpy (kJ/mol)	CO_2 uptake (mmol/g)	CO_2 uptake (mmol/cm^3)	BET surface (m^2/g)	selectivity
MOF-74 series	37−47	5.36−7.81	6.60−7.23	816−1495	182[b]
Cu-BTC	30	4.1	3.67	1571	~20
MoS_x aerogel	13−15	0.7[a]	N.A.	115−370	N.A.
$CoMo_3S_{13}$ chalcogel	6−13	0.9[a]	2.727[a]	569	N.A.
zeolite NaX	31−37	2.72	1.52	183	146[b]
zeolite 13X	40	4.70	3.24	726	30.4
Cs@RWY	30.2−32.1	3.21	5.84	526	180[a]
Rb@RWY	30.5−35.1	4.00	6.45	656	E.H.
K@RWY	35.0−41.1	4.98	6.86	716	E.H.

[a]Data collected at 273 K. [b]296 K and 1 atm. N.A. = not available. E.H. = extraordinarily high.

To test the recyclability of CO_2 adsorption of K@RWY, which exhibited the highest CO_2 uptake and the largest adsorption heat Q_{st} among these samples, the CO_2 gas adsorption isotherms were measured for eight cycles at 273 K and 1 atm. Between each cycle, the adsorbed CO_2 was readily removed under dynamic vacuum treatment for 2 h at room temperature. The results demonstrated that the uptake capacity was maintained over eight cycles, indicating a complete regeneration of this material through a facile process (Figure 4a).

The cation-exchanged zeolitic chalcogenides do have a strong tolerance toward water based on the fact that all of these samples were prepared in aqueous solutions. To further confirm the high stability, the K@RWY samples were directly soaked in water at RT and 313 K (40 °C) for 24 h (Figures S13−S14). The results shown in Figure 4b indicated that K@RWY still maintained a very high capacity after the regeneration process. In comparison, even under a less harsh condition, the CO_2 adsorption capacity of regenerated Mg-MOF-74 decreased significantly.[26]

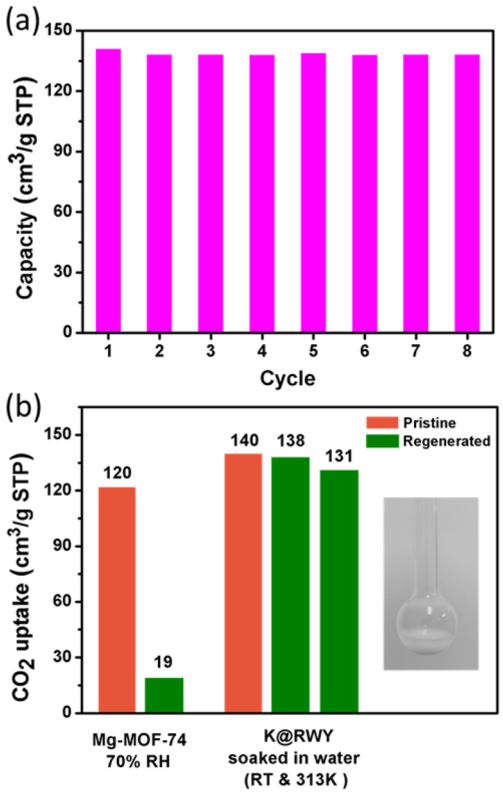

Figure 4. (a) Eight cycles of CO_2 uptake of K@RWY at 273 K and 1 atm. (b) CO_2 capacities of pristine Mg-MOF-74 and regenerated Mg-MOF-74 samples after hydration at 70% RH (data from ref 26) versus CO_2 capacities of K@RWY and regenerated K@RWY samples after soaking in water for 24 h at RT (left) and 313 K (right). The inset shows the picture of K@RWY soaking in water.

CONCLUSION

In summary, we have successfully synthesized a series of cation-exchanged samples through a postsynthetic stepwise ion-exchange strategy and evaluated their application in CO_2 adsorption. The results demonstrated that the samples of Cs@RWY, Rb@RWY, and K@RWY exhibited excellent CO_2 adsorption properties, which could be ascribed to the strong interaction between highly polarizable CO_2 and a "soft" electron-rich sulfur surface, as well as the interactions between extra-framework cations and CO_2. Particularly, the best performance was found in K@RWY with the highest uptake of 6.3 mmol/g at 273 K and 1 atm and the adsorption heat (35.0−41.1 mol^{-1}). More importantly, the N_2 adsorption of K@RWY under 298 K and even 273 K cannot be detected, which indicates an extraordinarily high CO_2/N_2 selectivity. Notably, it is also the best performance among all the reported chalcogenide materials. In addition, K@RWY also exhibited a good recyclability and a strong tolerance toward water.

ASSOCIATED CONTENT

Supporting Information

The Supporting Information is available free of charge on the ACS Publications website at DOI: 10.1021/acs.inorgchem.7b02307.

Additional information including structural representations, TG, EDS, etc. (PDF)

AUTHOR INFORMATION

Corresponding Authors

*E-mail: pingyun.feng@ucr.edu.
*E-mail: wutao@suda.edu.cn.

ORCID

Huajun Yang: 0000-0002-4664-4042
Min Luo: 0000-0001-8080-0881
Xiang Zhao: 0000-0001-7526-8261
Dongsheng Li: 0000-0003-1283-6334
Xianhui Bu: 0000-0002-2994-4051
Pingyun Feng: 0000-0003-3684-577X

DOI: 10.1021/acs.inorgchem.7b02307
Inorg. Chem. 2017, 56, 14999−15005

Tao Wu: 0000-0003-4443-1227

Author Contributions

[⊥]H.Y., M.L., and X.C. contributed equally to this work.

Notes

The authors declare no competing financial interest.

■ ACKNOWLEDGMENTS

We acknowledge the National Natural Science Foundation of China (T.W., 21671142), the Jiangsu Province Natural Science Fund for Distinguished Young Scholars (T.W., BK20160006), the Priority Academic Program Development of Jiangsu Higher Education Institutions (T.W., PAPD), and the NSF (P.F., DMR-1506661).

■ REFERENCES

(1) Lu, W.; Sculley, J. P.; Yuan, D.; Krishna, R.; Wei, Z.; Zhou, H. C. Polyamine-tethered porous polymer networks for carbon dioxide capture from flue gas. *Angew. Chem., Int. Ed.* **2012**, *51*, 7480−7484.

(2) Haszeldine, R. S. Carbon capture and storage: how green can black be? *Science* **2009**, *325*, 1647−1652.

(3) Rochelle, G. T. Amine scrubbing for CO_2 capture. *Science* **2009**, *325*, 1652−1654.

(4) Yu, K. M. K.; Curcic, I.; Gabriel, J.; Tsang, S. C. E. Recent advances in CO_2 capture and utilization. *ChemSusChem* **2008**, *1*, 893−899.

(5) Wang, Q.; Luo, J.; Zhong, Z.; Borgna, A. CO_2 capture by solid adsorbents and their applications: current status and new trends. *Energy Environ. Sci.* **2011**, *4*, 42−55.

(6) Xu, X.; Song, C.; Andresen, J. M.; Miller, B. G.; Scaroni, A. W. Novel polyethylenimine-modified mesoporous molecular sieve of MCM-41 type as high-capacity adsorbent for CO_2 capture. *Energy Fuels* **2002**, *16*, 1463−1469.

(7) Stuckert, N. R.; Yang, R. T. CO_2 capture from the atmosphere and simultaneous concentration using zeolites and amine-grafted SBA-15. *Environ. Sci. Technol.* **2011**, *45*, 10257−10264.

(8) Li, G.; Xiao, P.; Webley, P.; Zhang, J.; Singh, R.; Marshall, M. Capture of CO_2 from high humidity flue gas by vacuum swing adsorption with zeolite 13X. *Adsorption* **2008**, *14*, 415−422.

(9) Merel, J.; Clausse, M.; Meunier, F. Experimental investigation on CO_2 post-combustion capture by indirect thermal swing adsorption using 13X and 5A zeolites. *Ind. Eng. Chem. Res.* **2008**, *47*, 209−215.

(10) Liu, Q.; Cheung, N. C. O.; Garcia-Bennett, A. E.; Hedin, N. Aluminophosphates for CO_2 separation. *ChemSusChem* **2011**, *4*, 91−97.

(11) Deroche, I.; Gaberova, L.; Maurin, G.; Llewellyn, P.; Castro, M.; Wright, P. Adsorption of carbon dioxide in SAPO STA-7 and AlPO-18: grand canonical monte carlo simulations and microcalorimetry measurements. *Adsorption* **2008**, *14*, 207−213.

(12) Zhao, X. X.; Xu, X. L.; Sun, L. B.; Zhang, L. L.; Liu, X. Q. Adsorption behavior of carbon dioxide and methane on AlPO4−14: a neutral molecular sieve. *Energy Fuels* **2009**, *23*, 1534−1538.

(13) Lu, C.; Bai, H.; Wu, B.; Su, F.; Hwang, J. F. Comparative study of CO_2 capture by carbon nanotubes, activated carbons, and zeolites. *Energy Fuels* **2008**, *22*, 3050−3056.

(14) Hao, G. P.; Li, W. C.; Qian, D.; Lu, A. H. Rapid synthesis of nitrogen-doped porous carbon monolith for CO_2 capture. *Adv. Mater.* **2010**, *22*, 853−857.

(15) Dawson, R.; Stöckel, E.; Holst, J. R.; Adams, D. J.; Cooper, A. I. Microporous organic polymers for carbon dioxide capture. *Energy Environ. Sci.* **2011**, *4*, 4239−4245.

(16) Thallapally, P. K.; McGrail, B. P.; Atwood, J. L.; Gaeta, C.; Tedesco, C.; Neri, P. Carbon dioxide capture in a self-assembled organic nanochannels. *Chem. Mater.* **2007**, *19*, 3355−3357.

(17) McDonald, T. M.; D'Alessandro, D. M.; Krishna, R.; Long, J. R. Enhanced carbon dioxide capture upon incorporation of *N, N′*-dimethylethylenediamine in the metal-organic framework CuBTTri. *Chem. Sci.* **2011**, *2*, 2022−2028.

(18) McDonald, T. M.; Lee, W. R.; Mason, J. A.; Wiers, B. M.; Hong, C. S.; Long, J. R. Capture of carbon dioxide from air and flue gas in the alkylamine-appended metal-organic framework mmen-Mg_2 (dobpdc). *J. Am. Chem. Soc.* **2012**, *134*, 7056−7065.

(19) Mason, J. A.; Sumida, K.; Herm, Z. R.; Krishna, R.; Long, J. R. Evaluating metal-organic frameworks for post-combustion carbon dioxide capture via temperature swing adsorption. *Energy Environ. Sci.* **2011**, *4*, 3030−3040.

(20) D'Alessandro, D. M.; Smit, B.; Long, J. R. Carbon dioxide capture: prospects for new materials. *Angew. Chem., Int. Ed.* **2010**, *49*, 6058−6082.

(21) Sumida, K.; Rogow, D. L.; Mason, J. A.; McDonald, T. M.; Bloch, E. D.; Herm, Z. R.; Bae, T.-H.; Long, J. R. Carbon dioxide capture in metal-organic frameworks. *Chem. Rev.* **2012**, *112*, 724−781.

(22) Zhao, X.; Bu, X.; Zhai, Q.-G.; Tran, H.; Feng, P. Pore space partition by symmetry-matching regulated ligand insertion and dramatic tuning on carbon dioxide uptake. *J. Am. Chem. Soc.* **2015**, *137*, 1396−1399.

(23) Dunne, J.; Rao, M.; Sircar, S.; Gorte, R.; Myers, A. Calorimetric heats of adsorption and adsorption isotherms. 2. O_2, N_2, Ar, CO_2, CH_4, C_2H_6, and SF_6 on NaX, H-ZSM-5, and Na-ZSM-5 zeolites. *Langmuir* **1996**, *12*, 5896−5904.

(24) Liang, Z.; Marshall, M.; Chaffee, A. L. CO_2 adsorption-based separation by metal organic framework (Cu-BTC) versus zeolite (13X). *Energy Fuels* **2009**, *23*, 2785−2789.

(25) Zuluaga, S.; Fuentes-Fernandez, E. M.; Tan, K.; Xu, F.; Li, J.; Chabal, Y. J.; Thonhauser, T. Understanding and controlling water stability of MOF-74. *J. Mater. Chem. A* **2016**, *4*, 5176−5183.

(26) Kizzie, A. C.; Wongfoy, A. G.; Matzger, A. J. Effect of humidity on the performance of microporous coordination polymers as adsorbents for CO_2 capture. *Langmuir* **2011**, *27*, 6368−6373.

(27) Ori, G.; Massobrio, C.; Pradel, A.; Ribes, M.; Coasne, B. Nanoporous chalcogenides for adsorption and gas separation. *Phys. Chem. Chem. Phys.* **2016**, *18*, 13449−13458.

(28) Shafaei-Fallah, M.; Rothenberger, A.; Katsoulidis, A. P.; He, J.; Malliakas, C. D.; Kanatzidis, M. G. Extraordinary selectivity of $CoMo_3S_{13}$ chalcogel for C_2H_6 and CO_2 adsorption. *Adv. Mater.* **2011**, *23*, 4857−4860.

(29) Bag, S.; Kanatzidis, M. G. Chalcogels: porous metal-chalcogenide networks from main-group metal ions. Effect of surface polarizability on selectivity in gas separation. *J. Am. Chem. Soc.* **2010**, *132*, 14951−14959.

(30) Lin, Q.; Bu, X.; Mao, C.; Zhao, X.; Sasan, K.; Feng, P. Mimicking high-silica zeolites: highly stable germanium-and tin-rich zeolite-type chalcogenides. *J. Am. Chem. Soc.* **2015**, *137*, 6184−6187.

(31) Oh, Y.; Bag, S.; Malliakas, C. D.; Kanatzidis, M. G. Selective surfaces: high-surface-area zinc tin sulfide chalcogels. *Chem. Mater.* **2011**, *23*, 2447−2456.

(32) Shafaei-Fallah, M.; He, J.; Rothenberger, A.; Kanatzidis, M. G. Ion-exchangeable cobalt polysulfide chalcogel. *J. Am. Chem. Soc.* **2011**, *133*, 1200−1202.

(33) Armatas, G. S.; Kanatzidis, M. G. Mesoporous germanium-rich chalcogenido frameworks with highly polarizable surfaces and relevance to gas separation. *Nat. Mater.* **2009**, *8*, 217−222.

(34) Akhtar, F.; Liu, Q.; Hedin, N.; Bergström, L. Strong and binder free structured zeolite sorbents with very high CO_2-over-N_2 selectivities and high capacities to adsorb CO_2 rapidly. *Energy Environ. Sci.* **2012**, *5*, 7664−7673.

(35) Park, H. J.; Suh, M. P. Enhanced isosteric heat, selectivity, and uptake capacity of CO_2 adsorption in a metal-organic framework by impregnated metal ions. *Chem. Sci.* **2013**, *4*, 685−690.

(36) Dincă, M.; Long, J. R. High-enthalpy hydrogen adsorption in cation-exchanged variants of the microporous metal-organic framework $Mn_3[(Mn_4Cl)_3(BTT)_8(CH_3OH)_{10}]_2$. *J. Am. Chem. Soc.* **2007**, *129*, 11172−11176.

(37) Bae, T. H.; Hudson, M. R.; Mason, J. A.; Queen, W. L.; Dutton, J. J.; Sumida, K.; Micklash, K. J.; Kaye, S. S.; Brown, C. M.; Long, J. R. Evaluation of cation-exchanged zeolite adsorbents for post-combustion carbon dioxide capture. *Energy Environ. Sci.* **2013**, *6*, 128−138.

DOI: 10.1021/acs.inorgchem.7b02307
Inorg. Chem. 2017, 56, 14999−15005

(38) Zheng, N.; Feng, P. Microporous and photoluminescent chalcogenide zeolite analogs. *Science* **2002**, *298*, 2366−2369.
(39) Yang, H.; Luo, M.; Luo, L.; Wang, H.; Hu, D.; Lin, J.; Wang, X.; Wang, Y.; Wang, S.; Bu, X.; et al. Highly selective and rapid uptake of radionuclide cesium based on robust zeolitic chalcogenide via stepwise ion-exchange strategy. *Chem. Mater.* **2016**, *28*, 8774−8780.
(40) Myers, A. L.; Prausnitz, J. M. Thermodynamics of mixed-gas adsorption. *AIChE J.* **1965**, *11*, 121−127.
(41) Banerjee, D.; Zhang, Z.; Plonka, A. M.; Li, J.; Parise, J. B. A calcium coordination framework having permanent porosity and high CO_2/N_2 selectivity. *Cryst. Growth Des.* **2012**, *12*, 2162−2165.
(42) Lee, J.-S.; Kim, J.-H.; Kim, J.-T.; Suh, J.-K.; Lee, J.-M.; Lee, C.-H. Adsorption equilibria of CO_2 on zeolite 13X and zeolite X/activated carbon composite. *J. Chem. Eng. Data* **2002**, *47*, 1237−1242.
(43) Caskey, S. R.; Wong-Foy, A. G.; Matzger, A. J. Dramatic tuning of carbon dioxide uptake via metal substitution in a coordination polymer with cylindrical pores. *J. Am. Chem. Soc.* **2008**, *130*, 10870−10871.
(44) Subrahmanyam, K. S.; Malliakas, C. D.; Sarma, D.; Armatas, G. S.; Wu, J.; Kanatzidis, M. G. Ion-exchangeable molybdenum sulfide porous chalcogel: Gas adsorption and capture of iodine and mercury. *J. Am. Chem. Soc.* **2015**, *137*, 13943−13948.
(45) Millward, A. R.; Yaghi, O. M. Metal-organic frameworks with exceptionally high capacity for storage of carbon dioxide at room temperature. *J. Am. Chem. Soc.* **2005**, *127*, 17998−17999.
(46) Britt, D.; Furukawa, H.; Wang, B.; Glover, T. G.; Yaghi, O. M. Highly efficient separation of carbon dioxide by a metal-organic framework replete with open metal sites. *Proc. Natl. Acad. Sci. U. S. A.* **2009**, *106*, 20637−20640.

DOI: 10.1021/acs.inorgchem.7b02307
Inorg. Chem. 2017, 56, 14999−15005